A&A 519, A102 (2010)
DOI: 10.1051/0004-6361/201014819


Astronomy & Astrophysics

# The *Swift* Burst Analyser

## I. BAT and XRT spectral and flux evolution of gamma ray bursts

P. A. Evans[1], R. Willingale[1], J. P. Osborne[1], P. T. O'Brien[1], K. L. Page[1], C. B. Markwardt[2,3,4], S. D. Barthelmy[2], A. P. Beardmore[1], D. N. Burrows[5], C. Pagani[1], R. L. C. Starling[1], N. Gehrels[2], and P. Romano[6]

[1] Department of Physics and Astronomy, University of Leicester, Leicester, LE1 7RH, UK
e-mail: pae9@star.le.ac.uk
[2] NASA/Goddard Space Flight Center, Astrophysics Science Division, Greenbelt, MD 20771, USA
[3] CRESST/Center for Research and Exploration in Space Science and Technology, 10211 Wincopin Circle, Suite 500, Columbia, MD 21044, USA
[4] Department of Astronomy, University of Maryland College Park, College Park, MD 20742, USA
[5] Department of Astronomy and Astrophysics, 525 Davey Lab., Pennsylvania State University, University Park, PA 16802, USA
[6] INAF, Istituto di Astrofisica Spaziale e Fisica Cosmica, via U La Malfa 153, 90146 Palermo, Italy

Received 19 April 2010 / Accepted 15 June 2010

**ABSTRACT**

*Context.* Gamma ray burst models predict the broadband spectral evolution and the temporal evolution of the energy flux. In contrast, standard data analysis tools and data repositories provide count-rate data, or use single flux conversion factors for all of the data, neglecting spectral evolution.
*Aims.* We produce *Swift* BAT and XRT light curves in flux units, where the spectral evolution is accounted for.
*Methods.* We have developed software to use the hardness ratio information to track spectral evolution of GRBs, and thus to convert the count-rate light curves from the BAT and XRT instruments on *Swift* into accurate, evolution-aware flux light curves.
*Results.* The *Swift* Burst Analyser website⋆ contains BAT, XRT and combined BAT-XRT flux light curves in three energy regimes for all GRBs observed by the *Swift* satellite. These light curves are automatically built and updated when data become available, are presented in graphical and plain-text format, and are available for download and use in research.

**Key words.** gamma-ray burst: general – methods: data analysis – catalogs

## 1. Introduction

Gamma ray bursts are the most powerful explosions known, and the *Swift* satellite (Gehrels et al. 2004) has revolutionised our understanding of them, both in filling some gaps in our knowledge and raising new questions and challenges to theory. See Zhang (2007) for a recent review of GRBs and the advances made by *Swift*.

One of the difficulties inherent in confronting theory with the wealth of data that *Swift* has produced is that models predict how the flux and spectrum of a GRB or its afterglow will evolve, whereas the data are in units of count rate over some bandpass; in the presence of spectral evolution the count-rate cannot be seen as a proxy for the flux.

It is thus desirable to create GRB flux light curves[1] which employ a time-dependent flux conversion factor to account for spectral evolution. Also, since the bandpasses of the *Swift* Burst Alert Telescope (BAT; Barthelmy et al. 2005; bandpass: 15−350 keV) and X-ray Telescope (XRT; Burrows et al. 2005; bandpass: 0.3−10 keV), are close to each other, it is often informative to consider the two instruments' data together, extrapolated to a single bandpass, be it the XRT band (e.g. O'Brien et al. 2006; Willingale et al. 2007) or part of the BAT bandpass (e.g. 15−25 keV, Sakamoto et al. 2007).

We have therefore created the *Swift* Burst Analyser. In this first paper relating to the facility, we present an online repository of BAT and XRT unabsorbed flux light curves in three energy regimes: 0.3−10 keV flux, 15−50 keV flux, and the flux density at 10 keV. The Burst Analyser provides BAT and XRT flux light curves separately and combined; an example is shown in Fig. 1. It also includes a time evolution history for each instrument of the counts-to-flux conversion factor, and of the spectral photon index, $\Gamma$ (i.e. for a power-law spectrum with the number of photons at energy $E$ is given by $N(E)\mathrm{d}E \propto E^{-\Gamma}$). In addition, we provide BAT flux light curves where spectral evolution is not included, for comparison with the non-evolving XRT data already available online[2] (Evans et al. 2007, 2009). One example of the advantage of considering spectral evolution is shown in Fig. 2; for GRB 060729 the rapid decay phase is steeper when viewed in flux space with spectral evolution accounted for, which allows us to see the turn-on of the afterglow. (Note that Grupe et al. 2007, 2010 also accounted for spectral evolution in their analysis of this GRB. The evolution-induced dip feature shown in Fig. 2 is less prominant in the 0.3−10 keV band which is why it is not seen in their analysis.) We consider the physical interpretation of GRB light curves enabled by our new method in Paper II (Evans et al., in prep.).

⋆ http://www.swift.ac.uk/burst_analyser

[1] We create light curves in units both of flux and flux density; however for concision, we use the collective phrase, "flux light curves" to refer to both types.

[2] http://www.swift.ac.uk/xrt_curves

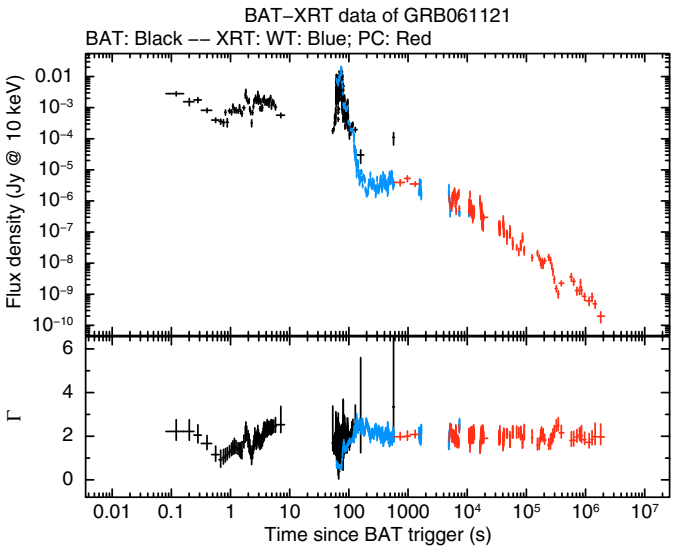


**Fig. 1.** An example of a flux density light curve from the Burst Analyser. The spectrally-evolving BAT-XRT flux light curve of GRB 061121, is shown as unabsorbed flux density at 10 keV; *the lower panel* shows the evolution of the photon index of the power-law spectrum. The last 3 BAT data points suffer from a poorly-constrained spectrum; see Sect. 3.4 for details.

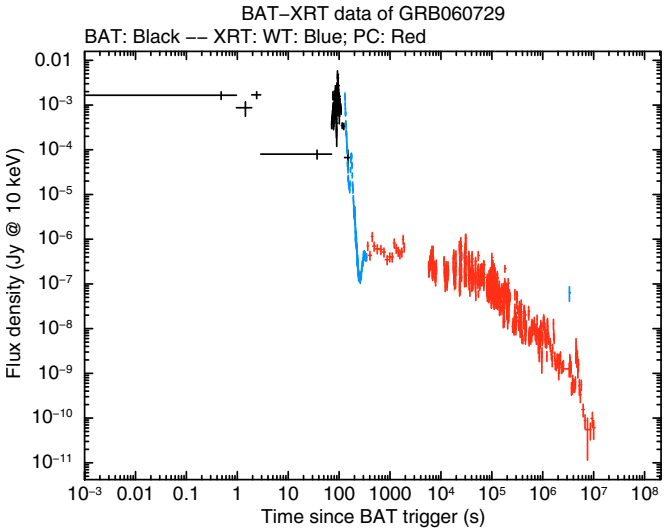


**Fig. 2.** The flux density light curve of GRB 060729 from the Burst Analyser. Accounting for spectral evolution shows the flux decline during the steep decay to be more rapid than in count space, and reveals the turn-on of the afterglow.

All of the data created by the Burst Analyser are available from: http://www.swift.ac.uk/burst_analyser. This includes graphical plots and the data in plain-text format.

In this paper we introduce the *Swift* Burst Analyser. In Sect. 2 we explain how the light curves are created and spectral evolution accounted for. Section 3 highlights the limitations of our method and some recommended checks users should apply. We also give details of when the light curves are created and how they can be accessed (Sect. 4), and the usage policy (Sect. 5).

## 2. Creation procedure

The process of creating the light curves comprises three phases: generating count-rate light curves and hardness ratios, determining the counts-to-flux conversion factors, and converting the count-rate light curves into flux units. Throughout the descriptions of thes phases, any FTOOLS used were called with the default parameters unless explicitly stated otherwise.

### 2.1. Count-rate light curves and hardness ratios

The XRT count-rate light curves used by the Burst Analyser are taken from the Swift XRT Light Curve Repository[2], and their creation has been documented in detail by Evans et al. (2007, 2009) and will not be repeated here. The hardness ratios are taken from the same place, but are first binned up to contain a minimum of 20 counts per band per bin (on the repository the minimum is 15 counts). This helps to reduce the effect of statistical fluctuations in the hardness ratio on the final light curve.

For BAT, the BATGRBPRODUCT script (part of the *Swift* software[3]) is first executed. Among the products created by this script are a measure of $T_{90}$ and the time range over which it was determined; a spectrum corresponding to this interval (hereafter, "the $T_{90}$ spectrum"); and an event list of BAT data extending to 2000 s either side of the trigger. From this event list a 4-ms binned 15−150 keV light curve is extracted using the BATBINEVT tool, supplied with relevant detector mask file created by BATGRBPRODUCT. Signal-to-noise-ratio (*SNR*)-binned light curves are built from this 4-ms light curve using a custom script. The "noise" on the input bins is the Poisson error in the count-rate (see the BAT Software Guide[4] for more information), and when rebinning the light curve this is propagated by adding in quadrature, as standard. The algorithm of the *SNR*-binning script is described below and illustrated in Fig. 3; in essence it bins the most significant parts of the light curve first, to maximise the time-resolution in those bins. In detail the algorithm is thus:

1. set $n = 1$;
2. bin the light curve (or light-curve sections) into new bins of $n$ original 4-ms bins. If any 4-ms bins are left over at the end of the light curve (or section), append them to the last new bin in the curve (or section);
3. search for any of these new bins with *SNR* above the threshold;
4. save any above-threshold new bins in the output light curve;
5. split the light curve into sections, separated by times which were saved to the output light curve in the previous step;
6. if at least one new above-threshold bin was found during this pass, increase $n$ by one; otherwise, double $n$;
7. if $n$ corresponds to a bin size of ≥40 s simply add every 40-s long bin to the output light curve;
8. if there are still bins in the original light curve which have not been assigned to the output light curve, go back to step 2. Otherwise, save the output light curve.

This results in a light curve in which bins are either above some *SNR* threshold, or 40 s in duration. This upper limit on bin size is set to preserve some information about the behaviour of the light curve during low-flux periods. Any bins which had $SNR < 3$ (regardless of the input *SNR* threshold) are flagged as unreliable, and not be shown in the online plots but they are included in the online data files (on lines beginning with an "!" – the comment-line delimiter for QDP). Using this above algorithm, light curves with *SNR* thresholds of 4−7 are created.

[3] http://swift.gsfc.nasa.gov/docs/software/lheasoft/download.html
[4] http://swift.gsfc.nasa.gov/docs/swift/analysis/bat_swguide_v6_3.pdf

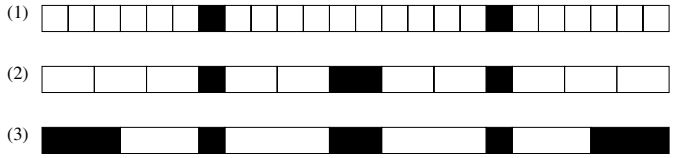


**Fig. 3.** A demonstration of the *SNR* binning algorithm. In the first pass (1) the bins marked in black were above the *SNR* threshold. For the second pass (2) the sub-threshold input bins were grouped in twos. One of these groups was found to be above threshold. In the third pass (3) the input bins were grouped in threes (with left-over input bins appended if necessary, meaning that some of the groups contain four input bins) and two of these were above threshold. This continues until all of the input bins are above threshold (i.e. the whole plot is black) or the input bins are grouped into new bins of 40-s or longer, at which point they are all added to the output light curve.

The BAT-XRT combined light curve will necessarily be presented in log-log space most of the time, thus data at $t \leq 0$ are not shown. Although one could simply use the light curve just created and ignore the bins before the trigger time, this will result in sub-optimal binning of the light curve. Instead a second set of light curves are built using the above algorithm, but given an input 4-ms-binned light curve which only contains data after the trigger time.

As well as the *SNR*-binned light curve, constant time-binned 15−150 keV light curves are also created, using BATBINEVT. These are nominally created for bin sizes of 4 ms, 64 ms, 1 s and 10 s, but if $T_{90} < 10$ s then the light curves with bin size longer than $T_{90}$ will not be built. Also, if $T_{90} > 10$ s the 4-ms binned light curve is not built, since this rapidly becomes extremely large. These light curves are accumulated only over the time range:

$$T_{90,\mathrm{start}} - 1.05T_{90} \leq t \leq T_{90,\mathrm{end}} + 1.05T_{90} \quad (1)$$

where $T_{90,\mathrm{start}}$ and $T_{90,\mathrm{end}}$ mark the time range over which $T_{90}$ was measured by BATGRBPRODUCT. This is to avoid filling the light curve with "empty" bins from times where the GRB was inactive.

A BAT hardness ratio defined as (25–50 keV)/(15–25 keV) is also created using the *SNR*-binning algorithm above, except that the *SNR* in *both* bands must be above the threshold before an output bin is created. The input 4-ms light curves in these bands are created with BATBINEVT. By default a hardness ratio with a *SNR* threshold of 5 is created. If this fails to produce at least two bins with $SNR \geq 3$ the threshold is reduced to 4, and if necessary further to 3. Even if there are still fewer than three bins with an $SNR \geq 3$ this hardness ratio will be used. The errors on the hardness ratio are calculated assuming that the individual bands' errors are Gaussian.

### 2.2. Counts-to-flux conversion factors

In order to convert the count-rate light curves (described above) into flux light curves, a time-evolving counts-to-flux conversion factor is needed. We do not have sufficient photons to create spectra with a reasonable time-resolution, so instead we assume a spectral shape and use the hardness ratios to track the evolution. GRB spectra tend to be power-laws, or broken power-laws. For the BAT data is has been found that sometimes a cut-off power-law best describes the data (Sakamoto et al. 2008).

We therefore fit the BAT $T_{90}$ spectrum with both power-law and cut-off power-law spectral models. If the latter gives a $\chi^2$ value at least nine lower than the former (i.e. a 3-$\sigma$ improvement) then a cut-off power-law model is used in all of the counts-to-flux conversion factor calculations (for BAT and XRT). This occurs for 15 per cent of GRBs; for the rest a power-law model is used. Note that using a single hardness ratio, we cannot track both the spectral index and the cut-off energy, but we lack the statistics to use multiple hardness ratios; we therefore keep the cut-off energy fixed at the value determined in the above fit, allowing no evolution of this parameter. This may introduce a systematic error or bias in our counts-to-flux conversion factors (hereafter "CF"), which is discussed in Sect. 3.2.

In addition to the emission model, an absorption model must also be determined. Following the XRT spectrum repository (Evans et al. 2009), we take the absorption model to consist of a PHABS component with the Galactic column density (from Kalberla et al. 2005) and a second PHABS component to represent the absorption local to the burst. If the redshift of the GRB is in the public domain, this component is a ZPHABS with the redshift of the GRB.

For GRBs with XRT data we can use the XRT data to determine the values of these absorption components. Butler & Kocevski (2007a) note that absorption derived from early-time XRT data, when strong spectral evolution is present, can be misleading. Therefore, if there are at least 200 X-ray photons detected at $T > 4000$ s post-trigger, a new spectrum is built using only the data from this time (using the software presented in Evans et al. 2009). If there are fewer than 200 late-time photons, the absorption values are taken from the XRT spectrum on the repository[5]. If there are no XRT data the Galactic absorption component is taken from Kalberla et al. (2005), and the intrinsic component is assumed to have $N_{\mathrm{H}} = 10^{22}$ cm$^{-2}$ and lie at $z = 2.23$; these being the mean values from the XRT catalogue (Evans et al. 2009). The absorption values used, and their provenance, are given on the Burst Analyser web page for each GRB.

The spectral model thus determined is loaded into XSPEC and the photon index of the (cut-off) power-law, $\Gamma$, is stepped from −1 to 5 in steps of 0.1. For each $\Gamma$ value the hardness ratio, unabsorbed 0.3−10 keV flux, unabsorbed 15−50 keV flux, model normalisation and count-rate predicted by the model are recorded[6]. This gives a look-up table of hardness ratio versus conversion factors (and $\Gamma$ values). The hardness ratios and count-rates are determined for the bands used in Sect. 2.1, i.e. for BAT the hardness ratio is (25−50 keV)/(15−25 keV) and the count-rate is determined over the 15−150 keV range. For XRT the hardness ratio is (1.5−10 keV/0.3−1.5 keV). The normalisation of the power-law and cut-off power-law models in XSPEC is defined as the flux density at 1 keV, in units of photons keV$^{-1}$ cm$^{-2}$ s$^{-1}$. A normalisation of one is thus equivalent to 662.5 $\mu$Jy. This can then be extrapolated to give the flux density at 10 keV using either:

$$F_{10\ \mathrm{keV}} = F_{1\ \mathrm{keV}} \times \left(\frac{10}{1}\right)^{-(\Gamma-1)} \quad (2)$$

for the power-law model, or

$$F_{10\ \mathrm{keV}} = F_{1\ \mathrm{keV}} \times \left(\frac{10}{1}\right)^{-(\Gamma-1)} \mathrm{e}^{-10/E_{\mathrm{c}}} \quad (3)$$

for the cut-off power-law, where $E_{\mathrm{c}}$ is the cut-off energy.

Given these look-up tables, the hardness ratios created in Sect. 2.1 can be converted instead into time evolution histories

[5] http://www.swift.ac.uk/xrt_spectra

[6] The count-rate is the observed, i.e. absorbed count rate.

**Table 1.** The phase spaces used to interpolate from hardness ratio (HR) to counts-to-flux conversion factors (CF) and spectral photon index (Γ).

| Instrument | 0.3–10 keV flux | 15–50 keV flux | 10 keV Flux density | Γ |
|---|---|---|---|---|
| BAT | log (HR), log (CF) | HR, CF | log (HR), log (CF) | log (HR), Γ |
| XRT | HR, CF | log (HR), log (CF) | log (HR), log (CF) | log (HR), Γ |

of conversion factors. For each bin in the original hardness ratio, the conversion factors and Γ value appropriate to that hardness are determined by interpolating within this lookup table. The uncertainties in the hardness are also propagated by interpolating the 1-$\sigma$ limits on the hardness ratios. For BAT data, because the bins may not exceed 40-s in duration, it is possible for some bins to have negative hardness ratios (from Poisson fluctuations of low significance bins). It is impossible for the lookup table to contain negative values, so these bins are skipped (and will be interpolated across in Sect. 2.3). Some bins may have positive hardness ratio values, but negative lower limits. In this case the error-bar on the conversion factor (or Γ) will be truncated at a hardness ratio tending to zero. See Sect. 3.4 for more information.

In order to make the (linear) interpolation as accurate as possible it is preferable to perform it in a phase-space that gives an approximately linear relationship between hardness ratio and the conversion factor. By inspecting look-up tables we thus chose the phase-spaces given in Table 1 for the interpolation.

For some GRBs, there were too few photons for even a single hardness ratio bin to be created for XRT. This is most commonly the case for bursts detected by missions other than *Swift*, which are often not observed by XRT until many hours after the trigger. In these cases Γ and the conversion factors were determined from the same spectrum used to obtain the absorption details (above); this does not allow for spectral evolution (see Sect. 3.5).

### 2.3. Flux light curves

For each bin in each count-rate light curve created in Sect. 2.1, a counts-to-flux conversion factor is determined by interpolating the time evolution histories of conversion factors created in Sect. 2.2. For BAT this interpolation is done in linear time space, for XRT log(time) space (since BAT includes negative times and a small time range, whereas XRT only has times after the trigger and covers many decades); the conversion factor is interpolated in log space for both instruments since it covers several decades. The count-rate and error are then multiplied by the conversion factor to give the flux for each bin. For BAT data, some hardness ratio bins with negative values of the ratio may have been skipped (Sect. 2.2) in which case the conversion factor is simply interpolated across this gap. Because GRBs show strong spectral evolution at early times, it is unwise to extrapolate the hardness ratio beyond times where we have a reliable measurement. Thus any light curve bins that occur after the end of the final valid (i.e. positive-valued) hardness ratio bin are discarded and not converted into flux. At later times the spectral evolution is minimal (Butler & Kocevski 2007b), thus for XRT any light curve bins which occur after the final hardness ratio bin are converted to flux using the conversion factors from the final hardness bin.

The uncertainty in the conversion factor is not propagated into the flux light curve. This is because it is in part a systematic effect and it will dilute the significance of genuine variability in the light curve. However, we require this information to determine whether features in the flux light curves are believable or not. Therefore, in addition to the basic flux light curve plots, we produce plots with subpanels showing either the conversion factor and its error, or the derived photon index (Γ) and its errors. Users can use these to consider how much weight should be applied to any given features.

As noted in Sect. 2.1, for BAT *SNR*-binned light curves the maximum permitted bin duration is 40 s, which can result in some low significance ($SNR < 3$) bins. These are not shown in the online plots, however they appear in the data files as lines beginning with an exclamation mark.

For BAT we also create a flux light curve with no spectral evolution (for XRT this is already provided by the Light Curve Repository). The creation is analogous to the light curves described above, but instead of using the hardness ratio to determine the conversion factor, a single conversion is used for all bins. This is taken from the model fitted to the $T_{90}$ spectrum. There are thus no sub-plots available for the non-evolving spectrum, instead the spectral model and conversion factors used are given on the Burst Analyser results page for each GRB.

## 3. Caveats and checks

Although substantial efforts have been made, by human analysis of the data products, to ensure that these products are reliable and accurate, there are some assumptions inherent to the light-curve creation process which may introduce artefacts. These are both predictable and identifiable. Several of the issues concern the uncertainty involved in extrapolating the BAT or XRT data beyond the range covered by the instrument; if there is any reason to question the assumptions involved in the light-curve creation process, we recommend that users consider the data in their "own" bands (i.e. the BAT data in the 15−50 keV range and the XRT data in the 0.3−10 keV range). For the combined BAT-XRT light curve the "safest" data to use is the flux density at 10 keV, as, for this dataset, the spectral extrapolation is minimal, as is the associated uncertainty.

In order to determine whether the data are reliable or potentially prone to inaccuracies, there are five questions that should be asked of a dataset.

### 3.1. Is Γ discontinuous between BAT and XRT?

An integral part of the flux conversion is the assumption of a spectral shape (Sect. 2.2). This can be a power-law or cut-off power-law, but in each case when the flux is extrapolated outside an instrument's bandpass (i.e. beyond the band over which the shape was determined) there is an implicit assumption that the power-law index remains the same. The temporal evolution of the photon index (Γ) as determined from the hardness ratios can be seen as a sub-plot on the light curves; the default display of the web pages shows this sub-plot. If the BAT and XRT data show discontinuous Γ values then the spectral shape changes between bands and the BAT flux extrapolated to the XRT band will be unreliable, and vice-versa. This discontinuity is present in about 20 per cent of cases. Although the flux density is not immune to this effect, is will be less strongly affected since it lies close to both bandpasses. This is demonstrated in Fig. 4.

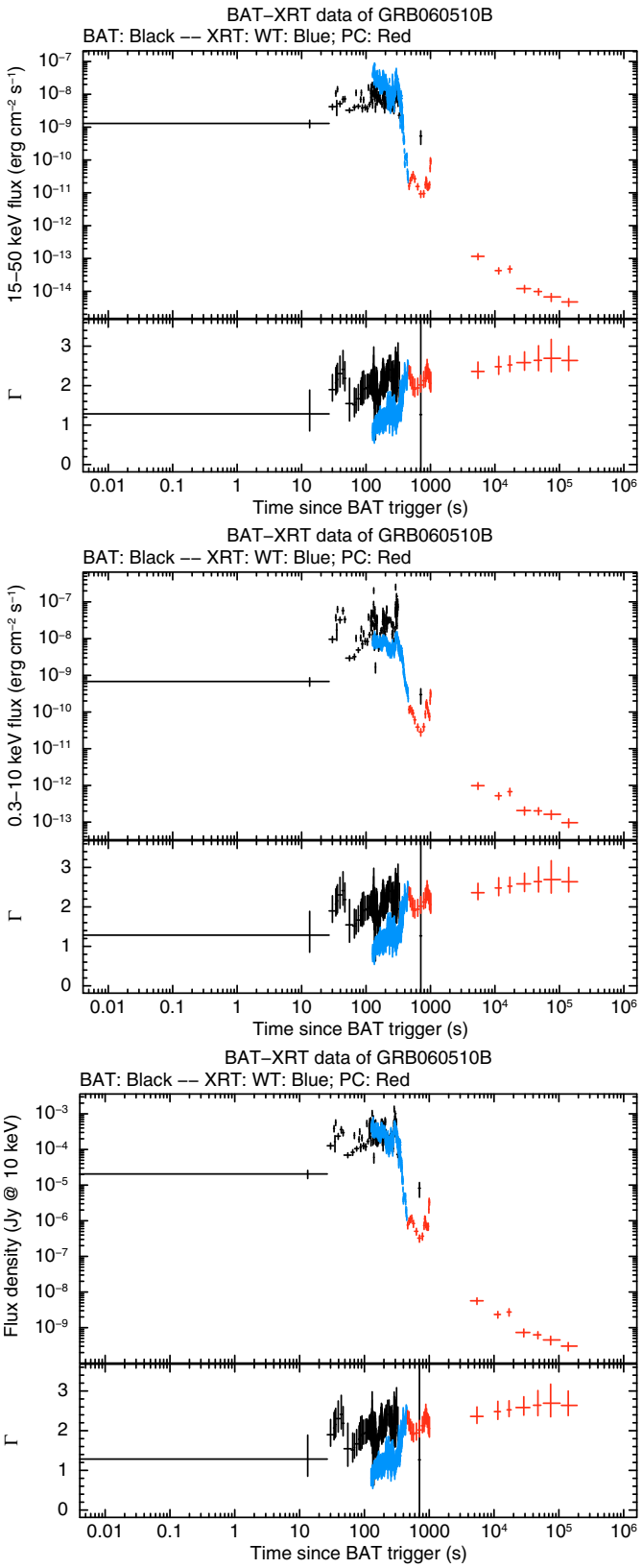


**Fig. 4.** Combined BAT-XRT light curve of GRB 060510B. The Γ panel shows that the BAT and XRT data are not joined by a single power-law spectrum, as is assumed when extrapolating the flux outside of the instruments' bandpasses. In the 15−50 keV band light curve (*top panel*) the XRT flux is overestimated compared to the BAT flux, and the inverse is true in the 0.3−10 keV light curve (*middle panel*). However as *the lower panel* shows, the 10 keV flux density light curve is much less vulnerable to this problem.

### 3.2. Is the BAT spectral fit a cut-off power-law?

As noted in Sect. 2.2, in some cases a cut-off power-law gives a better spectral fit than a power-law (in the 465 BAT light curves created for the Burst Analyser up to GRB 100316D, 67 required cut-off power-laws), however in these cases we do not allow the high-energy cut-off to vary. If the cut-off energy moves to lower energies with time, then at later times the flux above the cut-off will be overestimated; the inverse is true if the cut-off energy evolves to harder energies. To investigate the magnitude of this problem we created a series of BAT spectra for a range of Γ and cut-off energy ($E_c$) values. For each spectrum we determined the hardness ratio and count-to-flux conversion factors as in Sect. 2.2. Then, for each spectrum with a hardness ratio in the range 0.9−0.92 (i.e. spectra of approximately equal hardness), we show in Fig. 5 how the conversion factor and Γ necessary to generate such a hardness ratio vary with $E_c$. As can be seen, the $E_c$ dependence is not large (note the linear axes). For example, if $E_c$ was frozen at 80 keV, but in reality at late times it was 60 keV, the conversion factors would be inaccurate by up to 5 per cent. For more extreme examples of $E_c$ variation (e.g. from 80 keV to 40 keV) these inaccuracies can reach 50 per cent; however only when extrapolating outside of the BAT band. The conversion from BAT counts to 15−50 keV flux is never off by more than 2 per cent.

The range of cut-off energies is limited to 40−100 keV in Fig. 5 because at higher energies the 15−50 keV spectrum (whence the hardness ratio is obtained) is insensitive to the cut-off energy, and with lower values the hard band has so few counts that we cannot obtain a hardness ratio. For the XRT we do not see evidence for the cut-off power-law spectra, so freezing the cut-off energy should not affect the XRT flux conversions; except that if the cut-off energy were actually evolving through the 15−50 keV region the use of a fixed energy would lead to the XRT 15−50 keV flux values being overestimates.

In summary, for the ∼15 per cent of GRBs where a cut-off power-law is preferred to a power-law to fit the BAT spectrum, the flux extrapolated outside of the instruments' bandpasses may be subject to inaccuracies of a factor of at most two.

### 3.3. Are the Γ values outside the range 0–4?

Although there is considerable scatter in the Γ values found from BAT and XRT data, values outside the range ∼0−4 are not generally seen (see, for example, the Swift Data Table[7]; the BAT catalogue, Sakamoto et al. 2008; the XRT catalogue, Evans et al. 2009); thus if the Γ sub-plot shows values outside this range it may indicate a low *SNR* hardness ratio point rather than a real value of Γ and users should double-check the size of the errors on Γ and the conversion factor. Recall that the errors on the conversion factor are not propagated into the flux errors (see Sect. 3.4 for more). Most light curves show one or two bins with these "extreme" values; usually they are the last few bins in that BAT light curve and it is safe to disregard them.

Note also that the hardness-ratio-to-conversion-factor look-up table is only created for Γ values in the range −1 to 5; if a data point has a value outside of this range then the conversion factor has been extrapolated rather than interpolated, and may be less reliable.

[7] http://swift.gsfc.nasa.gov/docs/swift/archive/grb_table/

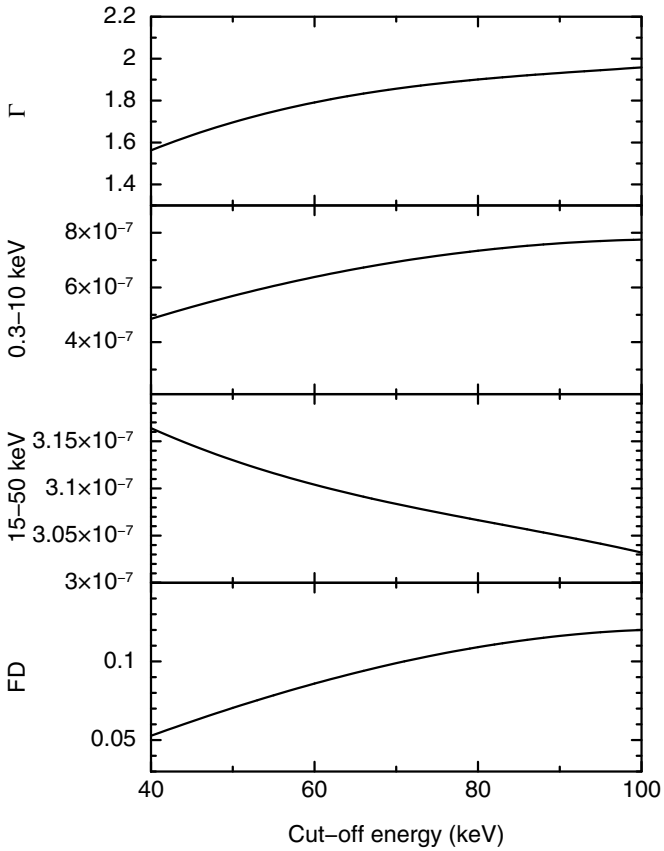


**Fig. 5.** The effect of the cut-off energy on the conversion factors and Γ value determined for a given hardness ratio. Panels (*top to bottom*) are the spectral index, counts-to-0.3−10-keV flux conversion factor, counts-to-15−150-keV flux conversion factor and counts-to-0.3−10-keV flux density conversion factor. See Sect. 3.2 for details.

### 3.4. Are the errors on Γ or the conversion factor large or asymmetric?

As discussed in Sect. 2.3, the uncertainty on the hardness ratio is propagated to the uncertainty on the conversion factor, but not into the final error-bar on the flux values. This is because, where the spectral evolution is not large, these errors are systematic in nature and tend to wash out genuine variability. However, if the errors on the conversion factor (visible in the sub-plots) are large compared to the actual flux values, users should not ascribe weight to apparently discrepant points. For example if a single data point lies significantly above the rest of the light curve and has a conversion factor which is inconsistent with the other conversion factor values and has a large error, the apparently discrepant flux is almost certainly the result of a poorly constrained spectral index, whose error is not reflected in the final light curve. To minimise confusion caused by these datapoints, any bin with "unreliable" conversion factors are not shown in the default online plots; in the datafile they are indicated by lines beginning with "!#". An "unreliable" conversion factor is defined as one where the error (positive or negative) is larger than two dex, or where the conversion factor is consistent with zero.

Because the hardness ratio errors were determined assuming Gaussian statistics in each BAT band, low *SNR* hardness bins can have negative error-bars which extend below zero. However, the hardness-ratio-to-conversion-factor look up table cannot contain negative hardness ratio values. Thus any datapoints corresponding to hardness ratios consistent with zero (i.e. non-detections in one of the bands) will have uncertainties on their Γ and conversion factor values which are truncated where the hardness ratio goes to zero. This can usually be spotted by a strongly asymmetric error on Γ or the conversion factor. Further, the hardness ratio and its corresponding Γ and conversion factors is viewable online and users can easily check if and when it becomes unreliable. There is no straightforward means of determining what the uncertainty in conversion factor should be at such times; it should instead be considered unconstrained and users are advised to ignore these datapoints. As with "extreme" values of Γ (Sect. 3.3), most light curves contain a few bins which are subject to this issue, typically at the end of the BAT data.

### 3.5. Do most/all of the bins for BAT or XRT have the same Γ or conversion factor value?

For low *SNR* datasets, there may be only one or two hardness ratio points. In this case the Γ sub-plots will show very little evolution. This is the case for ∼3 per cent of BAT light curves and ∼20 per cent of XRT light curves – many of the latter are GRBs detected by other missions which *Swift* did not observe until several hours after the trigger. For BAT-triggered GRBs, only 13 per cent of XRT hardness ratios have fewer than three bins. This is not a problem, it simply highlights a lack of information due to the low significance of the data, but users should note in this case that the light curves tend towards the non-evolving ones; we lack the data quality necessary to track the spectral evolution.

## 4. Data availability and creation policy

The data are all available online from: http://www.swift.ac.uk/burst_analyser/. The top-level page provides various means of choosing a specific burst, alternatively the trigger number or target ID of the object (if known) can be appended to the above URL.

The light curves exist both as plots (in postscript and png [Portable Network Graphics] format) and as text files. For each GRB there are up to four categories of light curve available: BAT-XRT combined data (only includes data after the trigger time), BAT-only data, XRT-only data, and a BAT light curve with no spectral evolution. For bursts where BAT or XRT data do not exist, not all of the above will be created. As discussed in Sects. 2.1 and 2.3 there are several different BAT-binning criteria used, and the light curves may have no sub-plot, or a panel showing the conversion factor or Γ value for each bin. Note that these values are the interpolated values; at the start of the four light curve sections is an option to view the *measured* hardness ratio, and its representation as Γ or conversion factors. Each light curve is also created in three different bands: the 0.3−10 keV flux, 15−50 keV flux, and flux density at 10 keV. The web page by default presents a single light curve (flux density, with a Γ sub-plot) for each of the categories, however users can change which plots are shown. As noted above, some BAT data points are considered unreliable, either from a low *SNR* (in the *SNR*-binned light curves), or because the uncertainty in the flux conversion is high. These are not shown in the default plot (alhough they are in the corresponding text file), however an option to show such points is given on the web pages. The conversion factor time evolution histories and a tar archive containing all of the data for the GRB in question are also available to download.

Full documentation supporting these web pages and downloadable files is also provided online at: http://www.swift.ac.uk/burst_analyser/docs.php. This page also contains a list of any changes made after publication of this paper.

The light curves are automatically created and updated via CRON jobs which run every ten minutes. These check both BAT and XRT data to determine whether products need to be built or updated. For BAT data the products will be built for the first time once data appear on on the quick-look site[8] (typically a few hours after the trigger), and updated when the ONTIME keyword of these data increases. For XRT data the products will be built or updated whenever the X-ray light curve from the Light Curve Repository[2] is created or updated.

Users can determine when a product was last updated from the web page for the GRB. At the top of the page, beneath the GRB name, are given details of the last dataset which was used to create the product. Also, in the footer bar at the base of the page, the time (in UT) when the page was last created is also specified.

## 5. Usage

The Burst Analyser data products are publically available and may be freely used. Users should consider the caveats in this paper (Sect. 3), and online (through the documentation link, above) before using the Burst Analyser data in any scientific medium.

Wherever these data products are used we ask that this paper be cited. The suggested wording is: "for details of how these light curves were produced, see Evans et al. (2010)".

Please also include the following paragraph in the Acknowledgements section: "this work made use of data supplied by the UK Swift Science Data Centre at the University of Leicester".

*Acknowledgements.* This work made use of data supplied by the UK Swift Science Data Centre at the University of Leicester. P.A.E., J.P.O., K.L.P., A.P.B., C.P. and R.L.C.S. acknowledge STFC support, D.N.B., acknowledges support from NASA contract NAS5-00136.

## References

Barthelmy, S. D., Barbier, L. M., Cummings, J. R., et al. 2005, Sp. Sci. Rev., 120, 143
Burrows, D. N., Hill, J. E., Nousek, J. A., et al. 2005, Sp. Sci. Rev., 120, 165
Butler, N. R., & Kocevski, D. 2007a, ApJ, 663, 407
Butler, N. R., & Kocevski, D. 2007b, ApJ, 668, 400
Evans, P. A., Beardmore, A. P., Page, K. L., et al. 2007, A&A, 469, 379
Evans, P. A., Beardmore, A. P., Page, K. L., et al. 2009, MNRAS, 397, 1177
Gehrels, N., Chincarini, G., Giommi, P., et al. 2004, ApJ, 611, 1005
Grupe, D., Gronwall, C., Wang, X.-Y., et al. 2007, ApJ, 662, 443
Grupe, D., Burrows, D. N., Wu, X.-F., et al. 2010, ApJ, 711, 1008
Kalberla, P. M. W., Burton, W. B., Hartmaan, D., et al. 2005, A&A, 440, 775
O'Brien, P. T., Willingale, R., Osborne, J., et al. 2006, ApJ, 647, 1213
Sakamoto, T., Hill, J. E., Yamazaki, R., et al. 2007, ApJ, 669, 1115
Sakamoto, T., Barthelmy, S. D., Barbier, L., et al. 2008, ApJS, 175, 179
Willingale, R. 2007, ApJ, 662, 1093
Zhang, B. 2007, ChJAA, 7, 1

[8] http://www.swift.ac.uk/access/ql.php